Journal of Inorganic Biochemistry 105 (2011) 31–38

Contents lists available at ScienceDirect

Journal of Inorganic Biochemistry

journal homepage: www.elsevier.com/locate/jinorgbio

A gallium complex with a new tripodal tris-hydroxypyridinone for potential nuclear diagnostic imaging: solution and *in vivo* studies of ^{67}Ga-labeled species

Sílvia Chaves [a], Ana C. Mendonça [a], Sérgio M. Marques [a], M. Isabel Prata [b], Ana C. Santos [b], André F. Martins [c], Carlos F.G.C. Geraldes [c], M. Amélia Santos [a,*]

[a] Centro de Química Estrutural, Instituto Superior Técnico-UTL, 1049-001 Lisboa, Portugal
[b] IBILI, Faculdade de Medicina, Universidade de Coimbra, Portugal
[c] Departamento de Ciências da Vida, Faculdade de Ciências e Tecnologia e Centro de Neurociências e Biologia Celular, Universidade Coimbra, 3001-401 Coimbra, Portugal

ARTICLE INFO

Article history:
Received 2 June 2010
Received in revised form 27 September 2010
Accepted 29 September 2010
Available online 7 October 2010

Keywords:
Hydroxypyridinones
Tripodal chelators
Gallium radioisotope
Biodistribution
Gamma scintigraphy
Gallium-67

ABSTRACT

The gallium(III) complex of a new tripodal 3-hydroxy-4-pyridinone (3,4-HP) chelator has been studied in terms of its physico-chemical and *in vivo* properties aimed at potential application as probe for nuclear imaging. In particular, based on spectrophotometric titrations, the hexa-coordinated (1:1) gallium complex appeared as the major species in a wide physiological acid-neutral pH range and its high stability (pGa = 27.5) should avoid drug-induced toxicity resulting from Ga(III) accumulation in tissues due to processes of transmetallation with endogenenous ligands or demetallation. A multinuclear (^{1}H and ^{71}Ga) NMR study gave some insights into the structure and dynamics of the gallium(III) chelate in solution, which are consistent with the tris-(3,4-HP) coordination and an eventual pseudo-octahedral geometry. Biodistribution and scintigraphic studies of the ^{67}Ga(III) labelled chelate, performed in Wistar rats, confirmed the *in vivo* stability of the radiolabelled complex, its non interaction with blood proteins and its quick renal clearance. These results indicate good perspectives for potential application of extrafunctionalized analogues in radio-diagnostic techniques.

1. Introduction

Gallium radioisotopes have been used for decades in diagnostic medicinal chemistry [1], although their importance has recently increased with the evolution of positron emission tomography (PET), namely after the advent of blended imaging devices (e.g. PET/CT, PET/MRI) which brought dramatic improvements by fusing functional and anatomical data [2].

The radioisotope ^{67}Ga ($t_{1/2}$ = 3.25 days) has long been recognized as an useful γ-emitter nuclide in conventional nuclear medicine scintigraphy or in single photon emission computed tomography (SPECT), for tumour and inflammation detection [1], while ^{68}Ga ($t_{1/2}$ = 68 min) labelled compounds have attracted much more attention due to their application in PET, combining suitable half-time for pharmacokinetics, high resolution, high sensitivity (down to picomolar) as well as the availability of a cost-effective generator and accessible chemistry [3,4]. Even though the most common PET radiolabelled compound is ^{18}F-FDG (18-fluorodeoxyglucose), it is reported to be of limited value for differentiation between various infectious and inflammatory conditions, and also it can only detect malignant cells with increased glucose metabolism [5,6]. Although ^{67}Ga-citrate has been mostly used in γ-scintigraphy, its limitations, namely due to nuclide binding to the plasma protein transferrin (resulting in relatively high background and therefore reduced lesion-to-background contrast), makes it less than ideal as an imaging agent. Thus, a number of complexes of ^{68}Ga with different ligands have been studied. The main requirement for those Ga(III) complexes to be used for diagnostic imaging is their high thermodynamic stability and kinetic inertness to avoid hydrolytic demetallation and also transmetallation by competitive blood serum ligands such as transferrin. Thus, polydentate ligands, such as the commercially available tetraaza-tetracetic acid DOTA derivatives (extrafunctionalized with specific peptides or other groups to account for targeting purposes), have been radiolabelled by coordination with ^{68}Ga and used in clinical trials [3,6,7]. Some further ligands, such as polyamino-polyacetate macrocycles (e.g. NOTA [8,9]), or other tripodal-based ligands (e.g. tris(salicylaldimine ligands [10]) have also been investigated. Among the commercially available compounds with amino-acetate chelating moieties, the tripodal derivatives have been less explored than the macrocyclic ones, mainly because of the higher inertness of macrocyclic complexes. However, that premised limitation could be overcome if a much stronger polydentate chelator is used. In fact, a new generation of gadolinium complexes with tripodal structure, namely Gd-(tris-1-hydroxy-2-pyridinone) complexes, have been recently proposed as contrast agents for magnetic resonance imaging (MRI) [11,12].

* Corresponding author. Tel.: +351 21 8419000; fax: +351 21 8464455.
E-mail address: masantos@ist.utl.pt (M.A. Santos).

0162-0134/$ – see front matter © 2010 Elsevier Inc. All rights reserved.
doi:10.1016/j.jinorgbio.2010.09.012

On the other hand, the similarity between Fe(III) and Ga(III), namely as hard Lewis acids with similar ionic radius, has raised the hypothesis of using strong iron chelators of the 3-hydroxy-4-pyridinone (HP) type, namely with bis- and tetra-denticity, for complexation with gallium aimed at potential radiodiagnostic applications [13,14].

Following our ongoing interest on searching for new strong polydentate HP for metal decorporation [15–17], we have recently developed a new series of very strong tripodal hexadentate-HP iron-chelators (see Scheme 1) [18]. Since these ligands can provide full hexadentate coordination for Ga(III), we decided to investigate one of those new tripodal HP (Scheme 1; NTP(PrHP)$_3$, p = 2, n = 1) for the Ga(III) complexation properties in aqueous solution as well as the *in vivo* behaviour. Thus, the thermodynamic stability of the gallium complexes and the corresponding speciation have been evaluated in solution by titrimetric methods, complemented by ligand protonation and structural information on the Ga(III) complex obtained by ^{1}H and ^{71}Ga NMR, while biodistribution and γ-scintigraphic studies of the corresponding ^{67}Ga(III) labelled chelates have been performed in Wistar rats. This study may be useful for the design of related tumour specific radiopharmaceuticals, namely with further N-functionalization, or eventually for dual-modality imaging (PET/MRI), assuming that the same ligand may also be a strong chelator for Gd(III).

2. Results and discussion

The new compound was prepared and characterized as reported in reference 18, namely in terms of acid–base properties in aqueous solution and lipo/hydrophilic character. The stepwise protonation constants are depicted in Table 1, which also includes the corresponding values for other tripodal compounds and deferiprone (DFP), aimed at comparative purposes. NTP(PrHP)$_3$ has seven dissociable protons (H_7L^{4+}), and the protonation constants (log K_i) depicted in Table 1 are assigned as follows: the first three values correspond to the three hydroxyl groups of the HP moieties; the fourth value is due to the backbone apical ammonium group; the last three values are attributable to the pyridinium protons of HP moieties [18]. This Table also includes the octanol/water partition coefficients (log P) for this ligand and other HP compounds at the physiological pH. This ligand presents a somewhat higher hydrophilic character (log P = −1.24) than KEMP-(HP)$_3$ derivatives (KEMP = *cis*, *cis*-1,3,5-cyclohexane-1,3,5-tricarboxylic acid [21] and the commercial chelator DFP (log P = −1.03), which is attributed to the apical protonated species (H_4L^+), that is reasonably abundant (ca 20%) at the physiological conditions (see Fig. 1).

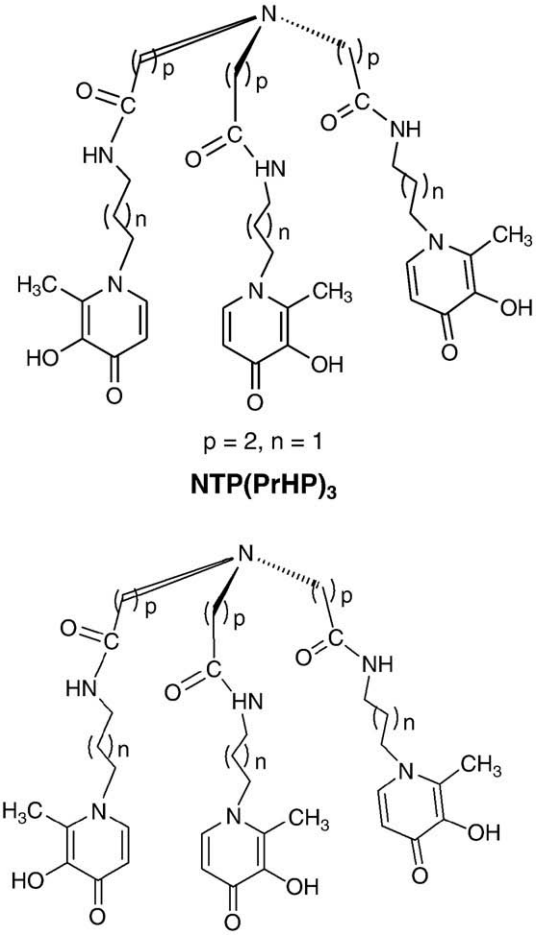

Scheme 1. Structural formula of the studied hexadentate 3,4-HP ligand.

2.1. Gallium complexation studies

The thermodynamic stability of the complexes of NTP(PrHP)$_3$ with Ga(III) in solution was evaluated herein and the calculated global stability constants are summarized in Table 1. Since the gallium-complex formation started below pH 2, the study of the Ga(III)/NTP(PrHP)$_3$ system required a spectrophotometric titration instead of a potentiometric technique. Thus, although the acid–base behaviour of the compound has already been studied by potentiometry [18], the spectral parameters for the different protonated species of the ligand were necessary for inclusion in the complexation model, and so a ligand spectrophotometric titration was also carried out.

Analysis of the distribution species diagram of NTP(PrHP)$_3$ as a function of pH (Fig. 1) shows that, for the range of pH between 4 and 6, the most abundant species is H_4L (90%) while for pH between 7.5 and 8.5 it is H_3L. The mono-positive ligand species (H_4L) has four protons attributed to the protonation of three hydroxyl groups and the apical nitrogen; in the H_3L species that nitrogen is deprotonated. At physiological conditions, the solution is a mixture of H_4L (20%) and H_3L (80%). The molar absorptivity values, specified in Fig. 1 and determined by spectrophotometric titration of the ligand, indicate that both H_4L and H_3L species absorb at λ = 280 nm, but not at 310 nm. In fact, these two wavelengths correspond to the absorption maxima for the chromophores of the protonated (H_iL) and deprotonated (L) hydroxypyridinone, respectively.

The global stability constants for the Ga(III) complexes of NTP(PrHP)$_3$ were determined from spectrophotometric titrations of the L/Ga(III) system at 1:1 ligand-to-metal ion molar ratio, which were carried out on two separate experiments (for pH ≤ 2 and pH > 2). Analysis of the speciation diagram of the gallium complexes as a function of pH (Fig. 2) reveals that the complex formation starts at pH < 2, thus suggesting for this ligand a strong affinity for Ga(III). Fig. 2 also indicates that, in the range of pH 1–2.5, the main species are GaH_iL (i = 5, 3). For the pH-range 3–5, the main species in solution is GaHL (90%), whereas at pH > 5.5 the neutral complex (GaL) becomes the predominant species. Above pH 6 there was some precipitation, which may be due to the formation of mixed (ligand-hydroxide)-Ga complexes. In fact, some degree of hydrolysis may already be present for pH > 5, explaining the fact that the pK value of GaHL (5.45) is slightly lower than log K_4 (6.77). Nevertheless, Fig. 2 evidences that both hexacoordinated complexes (GaHL and GaL, with neutral HP units) are present and absorb at λ = 299 nm, while the absorption at 278 nm should be due to high protonated species (GaH_5L and GaH_3L, with protonated HPs).

ESI-MS spectra of 1:1 solutions for the Ga(III)/NTP(PrHP)$_3$ (pH = 4.0) system confirmed the presence of the complex species $[GaHL)]^+$ (792.5).

Comparison between the metal (M) chelating affinities of ligands, with different proton dependency and denticity, is typically made on the basis of the corresponding pM values (pM = −log [M] with $C_L/C_M = 10$ and $C_M = 10^{-6}$ M at a specific pH), usually at the

Table 1
Stepwise protonation constants (log K_i) and partition coefficients (log P) for a set of tripodal compounds and DFP as well as the global formation constants (log β) of their Ga(III) complexes ($T = 25.0 \pm 0.1$ °C, $I = 0.1$ M KCl) and pGa*.

Ligand	log K_i	$Ga_pH_qL_r$ (p,q,r)	log β ($Ga_pH_qL_r$)	pGa	log P
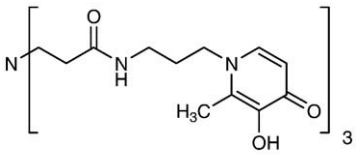 **NTP(PrHP)$_3$**	9.95[a] 9.84[a] 9.09[a] 6.77[a] 3.81[a] 3.14[a] 2.76[a]	(1,5,1) (1,3,1) (1,1,1) (1,0,1)	46.70(1) 44.00(4) 38.79(2) 33.34(3)	**27.5**	−1.24[a]
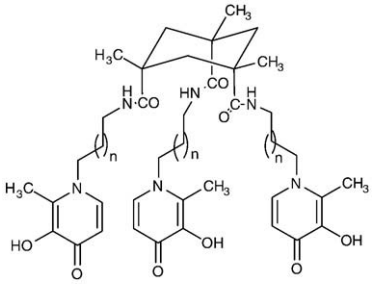 n = 1 **KEMP(PrHP)$_3$**	10.07[b] 9.89[b] 9.18[b] 3.98[b] 3.25[b] 2.91[b]	(1,4,1) (1,2,1)	41.00[b] 37.62[b]	–	−1.04[b]
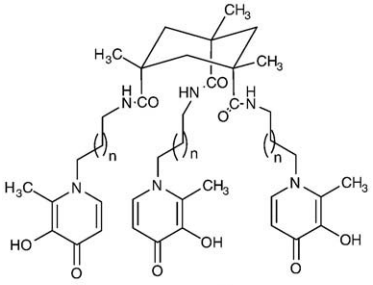 n = 2 **KEMP(BuHP)$_3$**	10.15[b] 9.91[b] 9.21[b] 4.05[b] 3.38[b] 3.10[b]	(1,4,1) (1,2,1)	41.78[b] 38.34[b]	–	−0.62[b]
DFP	9.77[c] 3.62[c]	(1,0,1) (1,0,2) (1,0,3)	13.17[c] 25.43[c] 35.76[c]	**17.8**	−0.85[a] −1.03[d]

*pGa values at pH = 7.4 ($C_{Ga} = 10^{-6}$ M, $C_L/C_{Ga} = 10$); numbers in brackets correspond to uncertainties provided by the PSEQUAD program for the fitting of 3 curves.
[a] Ref. [18].
[b] Ref. [17].
[c] Ref. [19].
[d] Ref. [20].

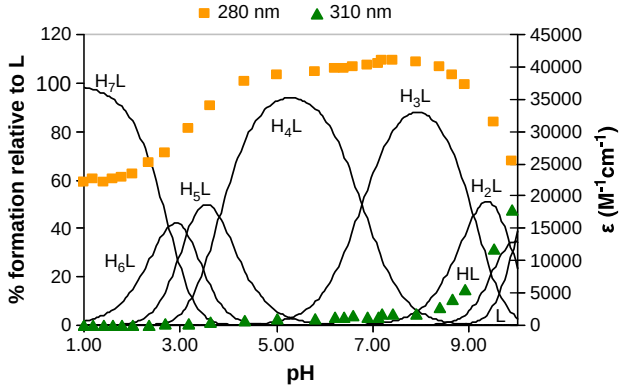

Fig. 1. Species distribution curves for NTP(PrHP)$_3$ with molar extinction coefficients at the maximum absorption wavelengths (b). ($C_L = 5.35 \times 10^{-5}$ M).

physiological pH (7.4). Therefore, pGa values were calculated for diverse Ga(III)-ligand systems, including the ligand in study and a set of synthetic ligands. For the Ga(III)/NTP(PrHP)$_3$ system, pGa value was determined admitting both that no precipitation prevailed at the diluted conditions of pM determination and also the maintenance of the complexation model. Analysis of pGa values for different systems, namely other hexadentate HPs or DFP, evidences the extraordinary high value (27.5) obtained for NTP(PrHP)$_3$. However, direct comparison between the stability of this gallium complex and the corresponding species with the KEMP(HP)$_3$ derivatives is herein impossible, at least on the basis of pGa values, because, due to insolubility problems found for the complexes of KEMP derivatives, the determination of the stability constant for the Ga-trischelate or the pGa values rendered impossible. Therefore, only a rough trend indication can be obtained for those values, on the basis of the first stepwise protonation constants of the corresponding complexes,

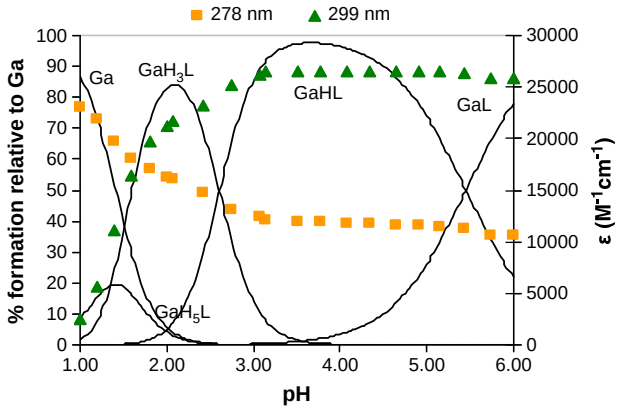

Fig. 2. Species distribution curves for the Ga(III)/NTP(PrHP)$_3$ system with molar extinction coefficients at the maximum absorption wavelengths ($C_L/C_{Ga}=1$, $C_L=5.2\times10^{-5}$ M).

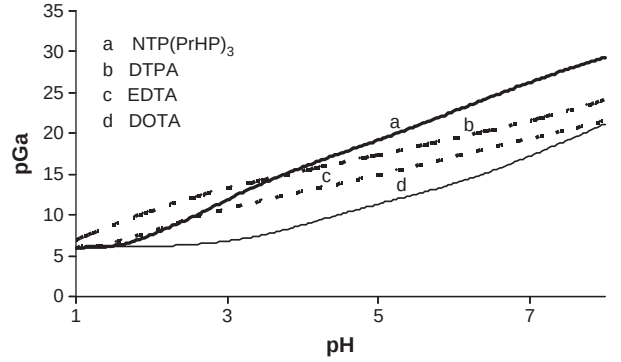

Fig. 3. pGa vs. pH plots for different Ga^{3+}/L systems (L = NTP(PrHP)$_3$, DTPA, EDTA, DOTA; $C_L/C_M=10$, $C_L=1\times10^{-5}$ M).

which seems to be slightly higher for the NTP(PrHP)$_3$ (3.7) than the KEMP(PrHP)$_3$ (3.4) chelates. Furthermore, a higher thermodynamic stability can be also expected for the NTP– than for the KEMP-gallium complexes based on comparison with the corresponding iron complexes. In fact the corresponding pFe values differed on ca 1-order of magnitude [18], and identical behaviour can be expected for gallium systems due to the similarity of the ionic radius of these three-charged metal ions (Fe, 65 pm; Ga, 62 pm). It is also clearly shown that, for the micromolar conditions that prevail in biological systems, the tris-chelator NTP(PrHP)$_3$ presents a much higher metal chelating efficacy than the monohydroxypyridinone derivative, DFP, due to its higher denticity. Moreover, comparison with previously published results also evidences that the thermodynamic stability of the Ga(III)-complexes with this new tris-HP ligand is even higher than with commercially available polyaminoacetate compounds that are used in diagnostic imaging, which pGa values are as follows: EDTA (20.2 [20]), DTPA (22.5 [22]) or DOTA (18.8 [22,23]). This is mainly ascribed to higher affinity of the hydroxypyridinone for gallium than the acetate chelating moieties, although for DOTA the macrocyclic effect may account for a higher kinetic stability.

The superiority of the thermodynamic stability of the Ga(III) complexes of the herein studied compound, as compared with other polydentate chelators, is also illustrated in Fig. 3. Furthermore, the high chelating capacity of NTP(PrHP)$_3$ towards gallium (pGa = 27.5), specially for pH above 4, should prevent transmetallation processes due to competition with endogenous ligands such as transferrin (pGa = 20.3 [24]), or even demetallation, thus avoiding drug-induced toxicity due to Ga(III) accumulation in tissues.

2.2. ^{1}H and ^{71}Ga NMR studies

The assignment of the eight non-labile proton resonances of the NTP(PrHP)$_3$ ligand in D_2O solution (Fig. S1) was assisted by 2D g-COSY spectra (Fig. S2), which showed vicinal cross-peaks between the HP proton doublets H_7 and H_8, the H_1 and H_2 protons of the NCH_2CH_2CO moieties, and between H_5 and H_4 and H_6 of the $NHCH_2CH_2$ CH_2N moieties of the three equivalent arms of the tripodal ligand. Fig. 4 shows the pH dependence of the chemical shifts of those proton resonances, assigned according to the numbering scheme shown for the NTP(PrHP)$_3$ ligand. This ^{1}H NMR titration curve is in agreement with the protonation constants of Table 1 and the macroscopic protonation scheme described above. This curve profiles appear associated to the effect that the protonation of each ligand basic site causes on the deshielding of the neighbour protons. The first three protonations at the three hydroxyl groups of the HP moieties deshield the H_7 and H_8 HP protons in the pH range 10–8. Then, protonation of the apical nitrogen atom deshields H_2 and H_1 in the pH range 8–6. Finally, the last three protonations at the pyridine nitrogen atom in the pH range 5–2 strongly deshield H_6 and to a lesser extent H_5 of the HP moieties, while H_7 and H_8 have an intermediate deshielding.

The ^{1}H NMR spectra of 5 mM Ga(III) and NTP(PrHP)$_3$ aqueous solutions, at pH 3.02, 7.04 and 9.01 (Fig. S3), are in good agreement

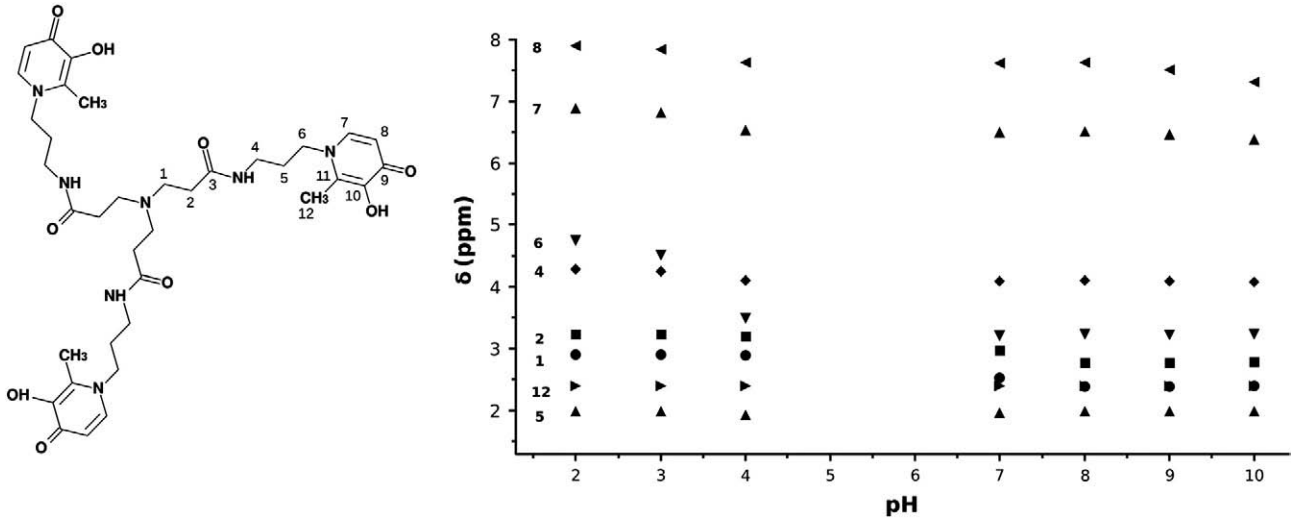

Fig. 4. pH dependence of the proton chemical shifts for NTP(PrHP)$_3$. Referencing of the non-labile proton resonances is according to the structure of the ligand shown on the left.

with the speciation diagram for the gallium complexes as a function of pH at 52 μM concentration described above (Fig. 2). At pH 3 the main species in solution, GaHL, gives eight sharp proton signals, indicating the presence of a single species with hexa-coordination and eventual pseudo-octahedral conformation. At pH 7, each of those protons gives multiple, but still relatively sharp resonances, thus reflecting the eventual formation of some mixed (ligand-hydroxide)-Ga complexes of low symmetry. None of these complexes give observable resonances in the ^{71}Ga NMR spectrum (data not shown), reflecting a very fast quadrupolar relaxation of the ^{71}Ga nucleus in an unsymmetrical coordination environment of a relatively large complex [25]. At pH 9, the broadening of the proton spectrum reflects the hydrolysis of the Ga(III) complex. A sharp ^{71}Ga resonance of the tetrahedral $Ga(OH)_4^-$ species at −170 ppm appears only at this pH value, indicating dissociation of the metal from the complex. Complex dissociation and precipitation was observed at a much higher concentration than that used in diagnostic imaging (μM), and at higher pH, and so precipitation problems should not occur for the *in vivo* conditions, as confirmed by experiments (see below).

2.3. Biodistribution studies and in vivo gamma imaging

The biodistributon data for the [^{67}Ga-NTP(PrHP)$_3$] complex, obtained at 30 min, 60 min and 24 h after intravenous injection (iv) in Wistar Rats, are expressed as the percentage of injected dose per gram of tissue (%ID/g) in Fig. 5. This radiolabelled complex exhibits rapid blood clearance during the first hour: at 60 min after injection only less than 2% of the injected dose stayed in the blood stream (considering that the blood corresponds to 7% of the body weight [26]). This result suggests that this compound doesn't interact with the serum proteins, such as serum albumin, which is in agreement with its global neutral charge. Thompson et al. [27] evaluated a series of gadolinium tripodal complexes and concluded that, besides some effect due to existence of aromatic structures, the interaction of a complex with serum albumin needs that the complex bears a negative charge that facilitates the interaction with the positively charged amino acid residues at the human serum albumin (HSA) binding site. At early times (30 and 60 min) the activity is located mainly in kidneys, blood and liver with almost no uptake in the other organs or tissues, considering that the small values of lung and heart activities correspond to circulating activity. Although at those times the main activity is found in kidneys, indicating the existence of a main renal excretion pathway for this hydrophilic complex, some liver uptake is also observable.

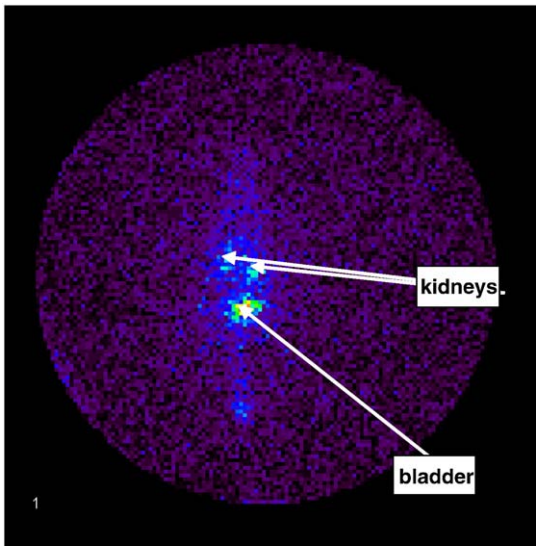

Fig. 6. Gamma scintigraphy image obtained 24 h after the injection of ^{67}Ga-NTP(PrHP)$_3$ in Wistar rats.

These observations agree with the gamma imaging findings. Although one would expect a higher liver (biliary) contribution for the excretion of these type of compounds bearing aromatic groups, in another similar study with gadolinium analogues [28] these authors claimed that the lipophilic/hydrophilic character play a more important role in the liver selectivity when compared to the existence of aromatic group substituents. From these studies we can also conclude that [^{67}Ga-NTP(PrHP)$_3$] doesn't pass the blood brain barrier due to its hydrophilic character.

The results of animal biodistribution agree with the gamma imaging data (Figs. 5 and 6). The time/activity curves obtained for the [^{67}Ga-NTP(PrHP)$_3$] from the dynamic acquisition experiments are

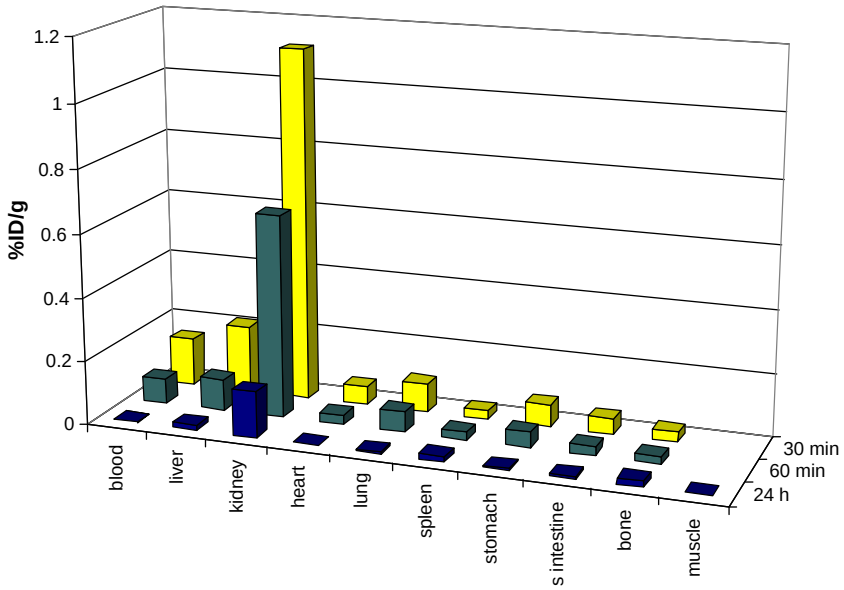

Fig. 5. Biodistribution study presented as percentage of injected dose per gram of organ (%ID/g) for ^{67}Ga-NTP(PrHP)$_3$ in Wistar rats (4–6 animals) at 30, 60 min and 24 h after intravenous injection.

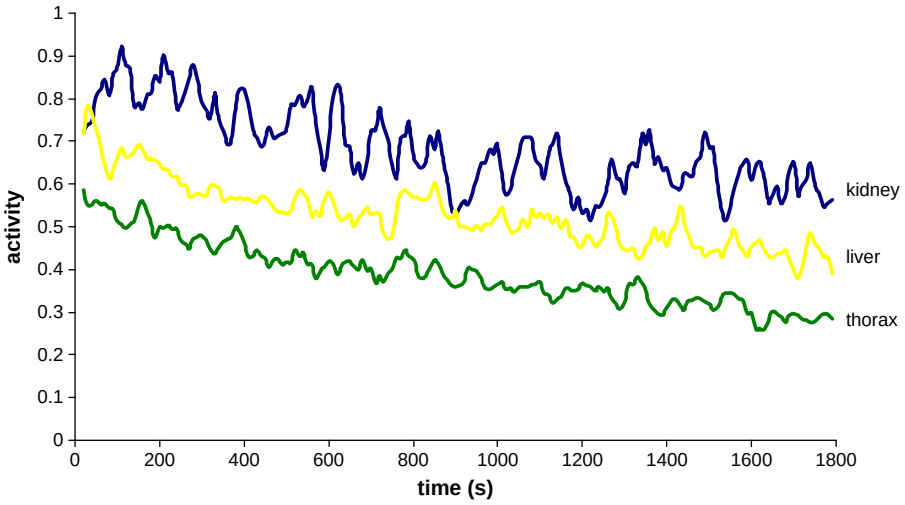

Fig. 7. Activity/time curves of ^{67}Ga-NTP(PrHP)$_3$ obtained from the dynamic images for the various regions of interest (kidneys, liver and thorax). The *YY* axis represents the normalized activity.

shown in Fig. 7. The curves were smoothed and normalized in relation to the maximum activity obtained.

Once again it is possible to observe that the clearance of this gallium complex occurs mainly through the kidneys. However, from these curves it can be also seen that the liver presents higher activities when compared with the thorax, which agrees with the biodistribution evidence of some liver uptake previously discussed. These results show again that almost all the radioactivity was cleared off from tissues and organs at 24 h and no significant deposition of the complex (or any $^{67}Ga^{3+}$-containing species) are observed in the liver–spleen region (see Figs. 6 and 7).

From the gamma imaging obtained at 24 h (Fig. 6) it is again noticeable that the main radioactivity comes from bladder, thus clearly indicating that the ^{67}Ga chelate underwent mostly renal clearance. The activity in the bones at 24 h, which is observed when the Ga(III)-transferrin complex is formed [29], is also very small (ca 0.02%).

These results evidence the high *in vivo* stability of the chelate, as expected from the fact that the thermodynamic stability of the complex is much higher than that for the complex of Ga^{3+} with transferrin (log $K = 20.3$) [24], which is the main competitor for Ga^{3+} in serum [12,24,30].

3. Conclusion

We have assessed the thermodynamic stability of the gallium complex with a new tripodal hexadentate tris-(3-hydroxy-4-pyridinone) (NTP(PrHP)$_3$) ligand and the biodistribution of the ^{67}Ga complex, aimed at potential application in radiodiagnostic imaging. The Ga(III) complexation studies in aqueous solution revealed for this compound a high Ga(III)-chelating efficacy by virtue of convenient pre-organization of three HP strong chelating units for metal wrapping and also for insulating it efficiently from competing bioligands, a relevant feature for medical applications. In fact, the pGa value for the Ga/NTP(PrHP)$_3$ system is higher than those of other commercially available compounds (EDTA, DTPA, DOTA, DFP) or even transferrin, with the concomitant reduced risk of toxicity due to transmetallation or demetallation processes. On the other hand, biodistribution studies of the [^{67}Ga-NTP(PrHP)$_3$] radiocomplex showed that it was mainly excreted through the kidneys and, after 24 h of injection, almost no radiation trace of the complex was found in the organism. Therefore, these studies point towards a potential application of NTP(PrHP)$_3$/Ga radiotracer chelate or other extra-functionalized analogues in important radiodiagnostic techniques such as PET imaging.

4. Experimental section

4.1. General remarks

The synthesis, the potentiometric protonation studies as well as the determination of partition coefficient (log *P*) of the ligand, NTP(PrHP)$_3$, were performed as previously described [18].

For the spectrophotometric studies performed herein, the electrode was calibrated by titration of a strong acid (HCl) solution with KOH solution and the results were analysed with Gran's procedure [31]. For the complexation studies, the $GaCl_3$ (4.16×10^{-3} M) solution was prepared in 0.1 M HCl (to prevent hydrolysis) from the respective gallium salt and standardized by inductively coupled plasma emission (ICP-AES) with a Jobin Yvon 38 Plus spectrometer. The exact HCl concentration was determined by standard addition method titration using 0.1 M HCl (Titrisol) for values of pH ≥ 2. The titrant was prepared from a carbonate-free KOH commercial solution (Titrisol) and standardized by titration with a potassium hydrogen phthalate solution. This solution was discarded whenever the percentage of carbonate (Gran's method [31]) was higher than 0.5% of the total amount of base.

Electronic spectra were recorded with a Perkin–Elmer Lambda 9 spectrophotometer, using 1 cm path length cells which were thermostated at 25.0 ± 0.1 °C by a Grant W6 equipment.

The mass spectra of the gallium complex were determined with a Varian 500-MS LC Ion Trap mass spectrometer equipped with an ESI ion source. The spray voltage was kept at 4.5 kV. The temperature of the heated capillary was set at 220 °C. The flow rate of the electrospray solution was 5 μL min^{-1}. Other parameters, including capillary voltage, lens and octapole voltages, and sheath gas flow rate were optimized for maximum abundance of the ions of interest.

4.2. Solution studies

4.2.1. Spectrophotometric measurements

The electronic spectra of NTP(PrHP)$_3$ (5×10^{-5} M) and of the respective 1:1 Ga(III)/NTP(PrHP)$_3$ system were recorded in the range 250–400 nm, in aqueous solution ($I = 0.1$ M KCl) and for pH > 2. Measurements for pH ≤ 2 were also performed, in the presence (1:1) and absence of the metal ion. For these titrations, the amount of acid to be added, from standard solutions (0.1 or 1 M HCl), was calculated in order to adjust the pH and obtain specific pH values (1, 1.2, 1.4, 1.6, 1.8 and 2.0).

4.2.2. Calculation of equilibrium constants

The stepwise protonation constants, $K_i = [H_iL]/[H_{i-1}L][H]$, and the overall gallium complex stability constants, $\beta_{M_mH_hL_l} = [M_mH_hL_l]/[M]^m[H]^h[L]^l$, were determined with the PSEQUAD program [32], by fitting of the spectrophotometric data and including the Ga(III) hydrolytic species ($\log \beta_{GaOH} = 11.4$, $\log\beta_{Ga(OH)_2} = 22.1$, $\log\beta_{Ga(OH)_3} = 31.7$, $\log\beta_{Ga(OH)_4} = 39.4$ [33]) in the equilibrium model. The value of K_w used in the computations was $10^{-13.77}$.

4.2.3. ^1H and ^{71}Ga NMR measurements

For NMR measurements, the solutions of the ligand $NTP(PrHP)_3$ and of its 1:1 Ga(III) complex were obtained by dissolving the appropriate amounts of $GaCl_3$ and ligand in D_2O (99.9% ^2H). The ^1H NMR spectra were assigned using the 1D presat and 2D g-COSY sequences. Proton 1D and 2D spectra were obtained at 298 K on a Varian VNMRS 600 spectrometer operating at 600.14 MHz. The ^1H chemical shifts are reported in ppm, relative to the tetramethylsilane (TMS) internal reference. ^{71}Ga NMR spectra were obtained on a Varian Unity 500 NMR spectrometer operating at 152.476 MHz, using the $[Ga(H_2O)_6]^{3+}$ signal at 0 ppm as external reference. The solution pH, corrected for the deuterium isotopic effect, was adjusted with diluted DCl and NaOD on a pH meter Crison micro TT 2050 with an electrode Mettler Toledo InLab 422. The pD values measured for the D_2O solutions were converted to the pH values using the deuterium isotopic correction pH = pD–0.4 [34–36].

4.3. Biodistribution studies

The complex [^{67}Ga-$NTP(PrHP)_3$] was prepared by dissolving the ligand (1 mg) in HEPES (200 μL, 0.1 M, pH 5) and by adding 1 mCi (1 Ci = 3.7×10^{10} Bq) of [^{67}Ga]citrate (purchased from CIS-BIO (Gif-sur-Yvette, France). Quality control was performed by TLC (eluent composition $CH_3CN/H_2O/NH_3$ 2:1:0.02). The radiochemical purity of the final product was higher than 98%.

Animal experiments were carried out with groups of four to six animals (Wistar male rats) weighing approximately 200 g. For the biodistribution studies, animals were anaesthetized with Ketamine (50 mg/mL)/chloropromazine (2.5%) (10:3) and injected in the tail vein (biodistribution at 24 h) or in the femoral vein (early biodistribution studies and imaging) with 100 μCi of the radiochemical and sacrificed 30 min, 60 min and 24 h later. The major organs were removed, weighted and counted in a γ well-counter.

4.4. In vivo gamma imaging

A gamma camera-computer system (GE 400 GenieAcq, from General Electric, Milwaukee, WI, USA) was used for acquisition and pre-processing. Data processing and display were performed on a personal computer using homemade software developed for the IDL 6.3 computer tool.

The animals were positioned in dorsal *decubitus* over the detector. Image acquisition was initiated immediately before the radiotracer injection. Sequences of 180 images (10 s each) were acquired to 64×64 matrices. In addition, static data were acquired 24 h after the radiotracer injection. Images were subsequently processed using an IDL based program (Interactive Data Language, Research Systems, Boulder, CO, USA). In order to analyze the transport of the radiotracer over time, three regions of interest (ROI) were drawn on the image files, corresponding to the thorax, liver and left kidney. From these regions, time–activity curves were obtained.

Abbreviations

COSY	COrrelation SpectroscopY
CT	computed tomography
DFO	desferrioxamine-B
DFP	Deferiprone
DOTA	1,4,7,10-tetraazacyclododecane-*N,N',N'',N'''*-tetraacetic acid
DTPA	diethylene triamine pentaacetic acid
EDTA	ethylenediaminetetraacetic acid
^{18}F-FDG	18-fluorodeoxyglucose
HEPES	4-(2-hydroxyethyl)-1-piperazineethanesulfonic acid
HP	hydroxypyridinones
3,4-HP	3-hydroxy-4-pyridinone
HAS	human serum albumin
ICP-AES	inductively coupled plasma atomic emission spectroscopy
ID	injected dose
Iv	intravenous injection
KEMP	cis,cis-1,3,5-cyclohexane-1,3,5-tricarboxylic acid
$KEMP(BuHP)_3$	1,3,5-tris-[4-(3-hydroxy-2-methyl-4-oxo-*4H*-pyridin-1-yl)-butylcarbamoyl]-1.3.5-trimethylcyclohexane
$KEMP(PrHP)_3$	1,3,5-tris-[3-(3-hydroxy-2-methyl-4-oxo-*4H*-pyridin-1-yl)-propylcarbamoyl]-1.3.5-trimethylcyclohexane
L	ligand
MRI	magnetic resonance imaging
NOTA	1,4,7-triazacyclononane-N,N',N''-triacetic acid
$NTP(PrHP)_3$	3,3',3''-nitrilotris(*N*-(3-(3-hydroxy-2-methyl-4-oxopyridin-1(4*H*)-yl)propyl)-propanamide)
PET	positron emission tomography
SPECT	single photon emission computed tomography
TLC	thin layer chromatography

Acknowledgments

The authors thank the Portuguese Fundação para a Ciência e Tecnologia (FCT) (projects PCDT/QUI/56985/04 and PTDC/QUI/70063/2006, PhD grant SFRH/BD/46370/2008 (A.F.M.), post-Doc grant SFRH/BPD/29874/2006 (S. M) and FEDER for the financial support. The mass spectra were obtained at the IST Node, which is part of the National Mass Spectrometry Network (RNEM) created by the Portuguese Foundation for Science and Technology (FCT). The Varian VNMRS 600 NMR spectrometer in Coimbra was acquired with the support of the Programa Nacional de Reequipamento Científico of the F.C.T., Portugal (contract REDE/1517/RMN/2005 – as part of RNRMN – Rede Nacional de RMN).

Appendix A. Supplementary data

Supplementary data to this article can be found online at doi:10.1016/j.jinorgbio.2010.09.012.

References

[1] C.J. Anderson, M.J. Welch, Chem. Rev. 99 (1999) 2219–2234.
[2] D.W. Townsend, J. Nucl. Med. 49 (2008) 938–954.
[3] H.R. Maecke, M. Hofmann, U. Haberkorn, J. Nucl. Chem. 46 (2005) 172S–178S 67-77.
[4] O.A.P. Breeman, M. de Jong, E. de Blois, B.F. Bernard, M. Konijnenberg, E.P. Krenning, Eur. J. Med. Mol. Imaging 32 (2005) 478–485.
[5] T.J. Mäkinen, P. Lankinen, T. Pöyhönen, J. Jalava, H.T. Aro, A. Roivainen, Eur. J. Nucl. Med. Mol. Imaging 32 (2005) 1259–1268.
[6] B.G. Conroy, N.D. Papathanasiou, V. Prakash, I. Kayani, M. Caplin, S. Mahmood, J.B. Bomanji, Eur. J. Med. Mol. Imaging 37 (2010) 49–57.
[7] D. Putzer, M. Gabriel, B. Henninger, D. Kendler, C. Uprimny, G. Dobrozemsky, C. Decristoforo, R.J. Bale, W. Jaschke, I.J. Virgolini, J. Nucl. Med. 50 (2009) 1214–1221.
[8] M. Fani, J.P. Andre, H.R. Maecke, Contrast Agents Mol. Imaging 3 (2008) 67–77.
[9] M.I.M. Prata, A.C. Santos, C.F.G.C. Geraldes, J.J.P. de Lima, Nucl. Med. Biol. 26 (1999) 707–710.
[10] M.K. Green, C.J. Mathias, W.L. Newmann, P.E. Fanwick, M. Janik, E.A. Deutsch, J. Nucl. Med. 34 (1993) 228–233.
[11] V.C. Pierre, M. Bota, S. Aime, K.N. Raymond, J. Am. Chem. Soc. 128 (2006) 5344–5345.
[12] E.J. Werner, A. Datta, C.J. Jocher, K.N. Raymond, Angew. Chem. Int. Ed. 47 (2008) 8568–8580.
[13] D.E. Green, C.L. Ferreira, R.V. Stick, B.O. Patrick, M.J. Adam, C. Orvig, Bioconjug. Chem. 16 (2005) 1597–1609.
[14] S. Gama, E. Farkas, P.I. Dron, S. Chaves, M.A. Santos, Dalton Trans. (2009) 6141–6150.
[15] M.A. Santos, Coord. Chem. Rev. 252 (2008) 1213–1224.
[16] M.A. Santos, Coord. Chem. Rev. 228 (2002) 187–203.

[17] R. Grazina, L. Gano, J. Sebestik, M.A. Santos, J. Inorg. Biochem. 103 (2009) 262–273.
[18] S. Chaves, S.M. Marques, A.M.F. Matos, A. Nunes, L. Gano, T. Tuccinardi, A. Martinelli, M.A. Santos, Chem. Eur. J. 16 (2010) 10535–10545.
[19] E.T. Clarke, A.E. Martell, Inorg. Chim. Acta 196 (1992) 185–194.
[20] R.A. Yokel, A.K. Datta, E.G. Jackson, J. Pharmacol. Exp. Ther. 257 (1991) 100–106.
[21] J. Rebek Jr., L. Marshall, R. Wolak, K. Parris, M. Killoran, B. Askew, D. Nameth, N. Islam, J. Am. Chem. Soc. 107 (1985) 7476–7481.
[22] A.E. Martell, R.M. Smith, R.J. Motekaitis, Critically selected stability constants of metal complexes database, Wiley, New York, 1997.
[23] E.T. Clarke, A.E. Martell, Inorg. Chim. Acta 190 (1991) 37–46.
[24] W.R. Harris, V.L. Pecoraro, Biochemistry 22 (1983) 292–299.
[25] J.W. Akitt, Multinuclear NMR, in: J. Mason (Ed.), Plenum Press, New York, 1987, pp. 259–292, Chapter 9.
[26] H.B. Lee, M.D. Blaufox, J. Nucl. Med. 25 (1985) 72–76.
[27] M.K. Thompson, D.M.J. Doble, L.S. Tso, S. Barra, M. Botta, S. Aime, K.N. Raymond, Inorg. Chem. 43 (2004) 8577–8586.
[28] M.K. Thompson, B. Misselwitz, L.S. Tso, D.M.J. Doble, H. Schmitt-Willich, K.N. Raymond, J. Med. Chem. 48 (2005) 3874–3877.
[29] J.F. Vallabhajosula, J.K. Harwig, N. Siemsen, W. Wolf, J. Nucl. Med. 21 (1980) 650–656.
[30] E. Thomas, Biochemistry 25 (1986) 4629–4633.
[31] F.J.C. Rossotti, H. Rossotti, J. Chem. Ed. 42 (1965) 375–378.
[32] L. Zékány, I. Nagypál, Computational Methods for the Determination of Stability Constants, in: D.J. Legget (Ed.), Plenum Press, New York, 1985.
[33] R.M. Smith, A.E. Martell, Critical Stability Constants, vol. 4, Plenum Press, New York, 1976 11.
[34] D.J. Alner, J.J. Greczek, A.G. Smeeth, J. Chem. Soc. A (1967) 1205–1211.
[35] K. Mikkelsen, S.O. Nielsen, J. Phys. Chem. 64 (1960) 632–637.
[36] P.K. Glasoe, F.A. Long, J. Phys. Chem. 64 (1960) 188–190.